S.J. Cox and G. Verbist

Liquid flow in foams under microgravity

The motion of liquid in aqueous foams under low gravity conditions is governed by diffusion equations. Two models of liquid behaviour are analyzed and solved, corresponding to the limits of slip and non-slip interfaces in the Plateau border network. The motion of wetting fronts is given in detail, to enable comparison with experiments performed in, for example, parabolic flights or in space. Both show similar behaviour, except for the sharpness of the wetting fronts. The experiments analyzed include the constant input of liquid into a foam at a point, and the wetting of a dry foam from a liquid reservoir.

1. Introduction

Foams are familiar materials, with widely known uses. The properties of aqueous foams are particularly well understood, at least in the limit of low liquid fraction [1]. Much of this understanding is due to the development of *drainage equations,* which describe the motion of liquid through a foam under various conditions [2, 3]. One of these conditions is the gravitational drainage which causes most of the liquid to leave the foam. In many applications, this drainage is undesirable. Consider for instance the fabrication of metallic foams [4, 5], in which a molten metal containing gas bubbles must be frozen before the metal drains out [6]. Eliminating gravity-driven drainage, by reducing the effect of gravity, would allow the production of metallic foams that have uniform density and therefore well-defined properties such as their buckling behaviour. With the advent of the International Space Station, an opportunity exists to study the behaviour of foams which are no longer subject to gravity. Foam experiments will soon be performed in space, and indeed some are already being performed in drop-towers and parabolic flights [7, 8, 9, 10, 11, 12]. To understand the results will require a new body of theory, and as a first step we propose to adapt the existing theory for aqueous foams under terrestrial gravity to fulfill this need. Note that this is actually a simplification of the theory, as described below. Another way of testing the theory experimentally may be possible under terrestrial gravity. The idea is to analyze in isolation the motion of liquid perpendicular to the direction of gravity, in two or three dimensions [13, 14], or to perform "horizontal" experiments in one or two dimensions. The flow of liquid through the foam in mutually perpendicular directions is uncoupled, so that the solutions to the zero-gravity drainage equations, which we shall derive here, are applicable to the horizontal liquid motion under terrestrial gravity. The first drainage equations were derived for a network of liquid channels, known as Plateau borders, in a foam [15]. The contribution of the soap films and of the junctions at which these borders meet was initially neglected. Within each border there must be a balance between the gravitational force on the liquid, the viscous dissipation on the walls, and the pressure difference caused by the curvature of the walls. With a condition of no-slip on the walls, i.e. assuming that these interfaces are rigid and the flow is of Poiseuille type, a relationship between the cross-sectional area of the channel and its position in the foam at some time is obtained [2, 16, 17]. The cross-sectional area of the Plateau borders is taken as a measure of the liquid fraction, the constant of proportionality being dependent upon the structure of the foam. Thus in what follows we try to extract scaling laws (for instance the motion of a wetting front with time), rather than exact quantities which will always be necessarily vague in the absence of a regular, known, bubble structure. Upon non-dimensionalization we are left with an equation of the form

$$\frac{\partial \alpha}{\partial \tau} + \nabla . \left(g\alpha^2 \hat{\xi} - \frac{\sqrt{\alpha}}{2} \nabla \alpha \right) = 0 \qquad \text{(rigid interfaces)} \qquad (1)$$

Mail adresses

S.J. Cox, Department of Physics, Trinity College, Dublin 2, Ireland.
G. Verbist, Shell Research and Technology Centre, PO Box 38000, 1030 BN Amsterdam, The Netherlands.
Email:simon.cox@tcd.ie
Paper submitted: 05.05.2003
Submission of final revised version: 10.10.2003
Paper accepted: 10.10.2003

where α is the Plateau border cross-sectional area, ∇ is the derivative operator with respect to position, τ is time and g is the acceleration due to gravity in the direction $\hat{\xi}$. The term in parentheses is the liquid flow-rate Q Several extensions and modifications to this model have been proposed. One approach is to include the effect of the Plateau border junctions as a correction to the length of the Plateau borders [18]. Koehler et al. [19] suggested that the no-slip condition on the walls of the Plateau borders is a poor approximation. They derived an alternative model, in which the interfaces in the foam are mobile, so that viscous dissipation occurs only in the junctions. This leads to a drainage equation of the form

$$\frac{\partial \alpha}{\partial \tau} + \nabla . \left(g\alpha^{3/2} \hat{\xi} - \frac{1}{2} \nabla \alpha \right) \qquad \text{(mobile interfaces)} \qquad (2)$$

Note that this differs from (1) only by a factor of $\sqrt{\alpha}$ in the flow-rate. It shares qualitatively the solutions of the equation for rigid interfaces, but shows a different scaling of the velocity of the liquid flow through a foam in relation to the input flow-rate Q_0 It is now widely accepted that these two models represent extremes of behaviour [20]. Their domains of applicability are still not fully understood, although they are known to depend upon bubble size and the chemical properties of the surfactant [21, 22]. Following the work of Leonard and Lemlich [15] and Kraynik [23], who recognized the importance of surface viscosity, Durand and Langevin [24] developed a drainage model that includes several contributions to the surface mobility in a single parameter. While this is undoubtedly the way forward, albeit given some doubts over the precise formulation and determination of the necessary coefficients, for ease of analysis we shall examine in the present work only the two limiting cases. This theory is based upon the liquid motion through the Plateau borders and their junctions, rather than the soap films, so that the continuum approximations inherent in the derivation mean that the equations should be applied to foams in which the bubble size is small compared to the dimensions of the container. For example, a one-dimensional (1D) analysis is often sufficient for a foam in a long narrow cylinder, and a two-dimensional (2D) analysis for small bubbles in a Hele- Shaw cell [13] - see figure 1. However, in 2D the equations should still give good predictions when the sample is only one bubble thick. This is because the liquid flows through the network of 2D Plateau borders on the surface of the foam sample, so that the only corrections to the theory are geometrical constants. Our goal then, is to extend the analysis [13, 25] of both the original foam drainage equation (1) and the more recent mobile-interfaces equation (2) in the case where the parameter g is zero. We neglect the case of varying gravity or of values of g between the two limits of micro- and terrestrial gravity (excluding, for example, any analysis pertinent to g-jitter). We also assume that $g = 1 \times 10^{-6}$, often given as the "actual" value of microgravity, is small enough compared to any gradient in liquid fraction that it can be neglected. Setting $g = 0$ in the drainage equations (1) and (2) gives

$$\frac{\partial \alpha}{\partial \tau} = \nabla . \left(\frac{\sqrt{\alpha}}{2} \nabla \alpha \right) \qquad \text{(rigid interfaces)} \qquad (3)$$

and

$$\frac{\partial \alpha}{\partial \tau} = \nabla . \left(\frac{1}{2} \nabla \alpha \right) \qquad \text{(mobile interfaces)} \qquad (4)$$

respectively. These are both diffusion equations; in the former case, the equation is nonlinear and will require considerably more effort to solve than the zero-gravity version of the equation for mobile interfaces, which is linear. In fact, the latter has several well-known solutions which we shall state without derivation. We shall in both cases exploit the self-similar scalings [26, 27] of these equations to assist in finding solutions. In fact the two equations are further related. If we were to linearize the zero-gravity drainage equation for rigid interfaces, for instance if we wished to follow the dynamics of a small disturbance in the liquid fraction α_0 of a wet foam, then we would find that the solutions found for the case of mobile interfaces apply, up to a constant factor of $\sqrt{\alpha_0}$. Of course, drainage is no longer an appropriate word in relation to the movement of liquid under zero-gravity. Instead we shall refer to it as diffusion or spreading, since it is exactly this process of liquid movement from wet to dry regions of the foam, caused by capillary forces, that the equations describe. It is evident then, that rather than the travelling wave fronts with constant profiles found under terrestri-

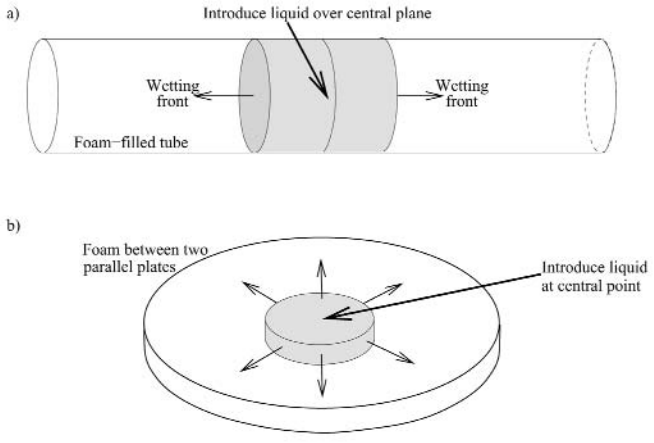

Figure 1: Sketches of the one- and two-dimensional geometries considered for pulsed and constant input. In each case dry foam fills the container and liquid is introduced over a small region. Wetting fronts, whose positions we wish to know, propagate in the directions indicated. a) A one-dimensional solution is applicable to liquid flow along the axis of a foam-filled tube. b) Two-dimensional solutions correspond to an axisymmetric situation in which foam between two parallel plates is invaded by liquid introduced at a point.

al gravity [28], we expect a slow smoothing of the profiles, with the purpose of spreading liquid evenly throughout the foam. All liquid motion therefore ceases when the liquid fraction is the same everywhere. In certain cases it will prove worthwhile to relate our dimensionless solutions to their dimensional counterparts. The relevant scalings differ considerably from those given elsewhere for the standard drainage equations [2, 3], so we give here the scalings for equations (3) and (4), and provide an estimate of the magnitude of the length- and time-scales. We denote the liquid surface tension by γ and its viscosity by η, assuming values for water containing surfactant: $\gamma = 2.5 \times 10^{-2}$ N/m and $\eta = 1 \times 10^{-3}$ Ns / m². Given the bubble volume V_b, we take a length-scale $x_0 = 2^{7/12}12^{-1/2}V_b^{1/3} \approx 0.43V_b^{1/3}$ that is approximately the length of a single Plateau border. This ensures that the liquid fraction Φ_t is numerically equal to α, with the reasonable but idealized assumption of a bubble structure consisting of Kelvin's regular tetrakaidecahedra. The time-scale is given by

$$t_0 = \frac{\eta x_0}{C\gamma K}$$

The geometrical constant

$$C = \sqrt{\sqrt{3} - \pi/2}$$

is related to the cross-sectional shape of a Plateau border, while the constant K depends upon the model. For rigid interfaces, analysis shows that $K = 6.6 \times 10^{-3}$, but for mobile interfaces a value of K must be inferred from experiment: we use $K \approx 2.3 \times 10^{-3}$ [3], although larger values were found in [29]. If we assume bubbles of volume $V_b = 1\text{mm}^3$ then $x_0 = 0.43$mm and $t_0 = 6.48 \times 10^{-3}$ s (rigid interfaces) and 1.86×10^{-2} s (mobile interfaces). We shall derive the necessary scaling solutions of the diffusion equations in § 2 before treating four cases: (i) the spreading of a small quantity of liquid (§ 3) introduced into the foam at time $\tau = 0$; (ii) the constant flow-rate input of liquid into the foam at a point (§ 4); the evolution of an initial step in liquid fraction (§ 5) and the movement of liquid into a dry foam which sits on a liquid pool (§ 6). We shall show that the significant difference between the solutions of the two equations, apart from the precise details of the scaling with time, is the nature of the wetting fronts that move through the foam. For the nonlinear case of rigid interfaces, the fronts between wet and dry foam are sharp. More precisely, the second derivative of liquid fraction with respect to position is non-zero at this point. On the other hand, the solutions for the liquid fraction in the case of mobile interfaces are exponential in form, so that they do not have a well-defined front. Thus a better way to characterize the spreading behaviour of the liquid in this case is to measure the width of the wet region, which grows with time. It may therefore prove easier to perform experiments with foams showing rigid interfaces, that is, with chemical properties that give non-slip interfaces.

2. Scaling solutions

We consider each of the zero-gravity diffusion equations in turn, and seek radially symmetric similarity solutions for $\alpha(\rho, \tau)$ where ρ is the radial distance from the origin. We are interested in analyzing experiments in one, two and three dimensions, so will consider the general case of d dimensions.

2.1 Case of rigid interfaces

The relevant nonlinear diffusion equation is (3) which we write

$$\frac{\partial \alpha}{\partial \tau} = \frac{1}{2\rho^{d-1}} \frac{\partial}{\partial \rho}\left(\rho^{d-1} \sqrt{\alpha} \frac{\partial \alpha}{\partial \rho} \right) \tag{5}$$

$$= \frac{1}{3\rho^{d-1}} \frac{\partial}{\partial \rho}\left(\rho^{d-1} \frac{\partial}{\partial \rho}\left(\alpha^{3/2} \right) \right) \tag{6}$$

This admits solutions of the form

$$\alpha(\rho, \tau) = \tau^{(4-2m)/m} y(s), \qquad s = \frac{\rho}{\tau^{1/m}} \tag{7}$$

where the integer m is found from the relevant boundary conditions for each experiment of interest. In each case the wetting front moves as $\rho_0 \sim \tau^{1/m}$ and the motion of the point of maximum liquid fraction varies according to $\alpha \sim \tau^{(4-2m)/m}$. The similarity function $y(s)$ satisfies

$$\frac{6(m-2)s^{d-1}}{m} y + \frac{s^d}{m} y' + (s^{d-1}(y^{3/2})')' = 0 \tag{8}$$

where primes denote derivatives with respect to s. To complete the specification of the problem we require a second boundary condition. In all cases considered here, we shall assume the presence of a sharp wetting front at $\rho = \rho_0(t)$, so we choose $\alpha(\rho, \tau) = 0 \; \forall \; \rho \geq \rho_0$.

2.2 Case of mobile interfaces

In this case we write the diffusion equation (4) as

$$\frac{\partial \alpha}{\partial \tau} = \frac{1}{2\rho^{d-1}} \frac{\partial}{\partial \rho}\left(\rho^{d-1} \frac{\partial \alpha}{\partial \rho} \right) \tag{9}$$

$$= \frac{1}{2}\left(\frac{\partial^2 \alpha}{\partial \rho^2} + \frac{d-1}{\rho} \frac{\partial \alpha}{\partial \rho} \right) \tag{10}$$

which admits solutions of the form

$$\alpha(\rho, \tau) = \tau^{n/2} y(s), \qquad s = \frac{\rho}{\tau^{1/2}} \tag{11}$$

showing that the wet regions of the foam expand with $\rho \sim \tau^{1/2}$. The maximum liquid fraction decreases as $\tau^{n/2}$, where the integer n will be found for each of the boundary conditions considered. For the second boundary condition we no longer expect a sharp wetting front, so since the liquid fraction is initially zero we assume that $\alpha \to 0$ as $\rho \to \infty$. The similarity function $y(s)$ satisfies

$$-ns^{d-1} y + s^d y' + (s^{d-1} y')' = 0 \tag{12}$$

We shall describe solutions to this equation in the following sections.

3. A spreading pulse

The diffusion of an initially localized volume of liquid throughout a foam under zero gravity has already been studied [13, 16, 25, 30]. We shall provide a brief review of the main results, and have used it to verify the numerical code used below to provide visualizations of the liquid movement. A small volume λ_0 of liquid is introduced into a dry foam (with α=0) and left to spread. This volume of liquid must be conserved, so that we have the condition:

$$\lambda_0 = \int_0^{\rho_0} c_d \rho^{d-1} \alpha \, d\rho \tag{13}$$

where $c_d = 2, 2\pi, 4\pi$ for $d = 1, 2, 3$ respectively.

3.1 Case of rigid interfaces

The conservation of liquid condition (13) gives m=1/2(d+4) so that [25]

$$\alpha(\rho,\tau) = \tau^{-2d/(d+4)} y(s), \qquad s = \frac{\rho}{\tau^{2/(d+4)}} \tag{14}$$

Equation (8) for $y(s)$ becomes

$$6ds^{d-1} y + 6s^d y' + (d+4)(s^{d-1}(y^{3/2})')' = 0 \tag{15}$$

with solution

$$y(s) = \left(c - \frac{s^2}{d+4} \right)^2 \tag{16}$$

for a constant c which is given by conservation of liquid (13). Then

$$\alpha(\rho,\tau) = \begin{cases} \tau^{-2d/(d+4)} \left(c - \dfrac{\rho^2}{(d+4)\tau^{4/(d+4)}} \right) & \rho^2 \le c(d+4)\tau^{4/(d+4)} \\ 0 & \rho^2 \ge c(d+4)\tau^{4/(d+4)} \end{cases} \tag{17}$$

where

$$c = \left(\frac{d(d+2)(d+4)^{1-d/2} \lambda_0}{8 c_d} \right)^{2/(d+4)} \tag{18}$$

The liquid fraction at the origin is therefore given by α=$\tau^{-2d/(d+4)}c^2$, increasing with the liquid volume as $\lambda_0^{4/(d+4)}$. Similarly, the front is found at position

$$\rho_0 = \sqrt{c(d+4)}\,\tau^{2/(d+4)} \tag{19}$$

which increases with the liquid volume as $\lambda_0^{1/(d+4)}$.

3.2 Case of mobile interfaces

With the linear diffusion equation (10), we find that for a quantity λ_0 of liquid, the constant n is equal to $-d$ so that the liquid fraction α scales according to

$$\alpha(\rho,\tau) = \tau^{-d/2}(y/s), \qquad s = \frac{\rho}{\tau^{1/2}} \tag{20}$$

That is, the pulse widens with the square root of time and the point of maximum liquid fraction at $\rho = 0$ decreases with $\tau^{-d/2}$. We must then solve the following ODE for $y(s)$, from (12):

$$ds^{d-1} y + s^d y' + (s^{d-1} y')' = 0 \tag{21}$$

The solution takes the form of a Gaussian [13]:

$$\alpha(\rho,\tau) = \frac{\lambda_0}{(2\pi\tau)^{d/2}} \exp\left(-\frac{\rho^2}{2\tau} \right) \tag{22}$$

In this case the liquid fraction at the origin increases in linear proportion to the volume of liquid added, whereas this volume doesn't affect the position of the front.

3.3 Dimensional comparison of pulse profiles

In figure 2 we show 2D solutions for a spreading pulse in each case. We consider a foam between two parallel plates, sketched in figure 1b), a distance H = 10mm apart and at time t = 0 introduce a uniform cylinder of liquid of volume V_0 = 10mm^3 which spans the gap at r = 0. The figures show profiles of liquid fraction for various times in the evolution of a pulse. To obtain these profiles in dimensional variables, we scale the radial position to get $r = \rho x_0$ and put time $t = t_0 \tau$ using the quantities defined in the introduction. The volume of liquid is $V_0 = x^2_0 H \lambda_0$. The position of the front in the case of rigid interfaces is given by $r_0 = 0.0055\, t^{1/3}$ while the width (standard deviation) of the Gaussian increases as $r_0 = 0.0032\, t^{1/2}$, showing that the latter will grow more quickly after some time. Similarly, the height of the pulse decreases less quickly ($0.0031/t^{2/3}$ compared to $0.016/t$) for rigid interfaces.

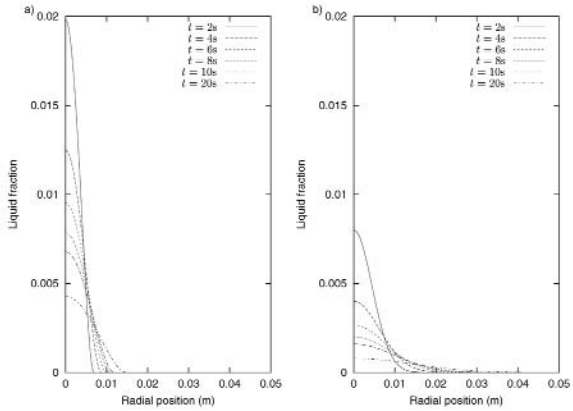

Figure 2: The zero-gravity spreading of a pulse of liquid introduced into a dry 2D foam between two parallel plates. Profiles of liquid fraction are shown at various times t, from an initial volume of liquid V_0=10mm³ . a) The case of rigid interfaces, with solution given by (17). b) The case of mobile interfaces, from (22). Notice the more rapid decrease in the height of the pulse in the second case, and its consequent rapid spreading. With rigid interfaces, however, there is a sharp front.

4. Constant input of liquid

In this experiment we start with a foam which has vanishing liquid fraction everywhere, $\alpha = 0$. Liquid is then added with constant flow-rate at $\rho = 0$, so that the foam becomes progressively wetter. In 1D this corresponds to a long tube filled with foam, into which liquid is continuously injected at the centre through a small hole in the wall of the tube, shown in figure 1a.

4.1 Case of rigid interfaces

The flow-rate is the term in parentheses in (3):

$$Q = -\frac{1}{2}\sqrt{\alpha}\nabla\alpha = -\frac{1}{3}\frac{\partial}{\partial\rho}\left(\alpha^{3/2}\right) \tag{23}$$

The scaling parameter m is found by considering the flow-rate $Q_0 = c_d \rho^{d-1} Q\big|_{\rho=0}$ to be constant in time. Then m = 1/3 (d+4) so that

$$\alpha(\rho,\tau) = \tau^{2(2-d)/(d+4)}(y/s), \qquad s = \frac{\rho}{\tau^{3/(d+4)}} \tag{24}$$

Notice the behaviour of the liquid fraction at the point of input: in 1D it *increases* with time, while in 3D it *decreases* - thus liquid diffuses away faster than it is introduced in a 3D foam. The interesting case, and probably the easiest to verify experimentally, is in 2D, where the liquid fraction at the point of input is *constant*. The wetting front moves away from the origin at a rate proportional to $\tau^{-3/(d+4)}$. Substitution in (8) shows that $y(s)$ satisfies

$$6(d-s)s^{d-1}y + 9s^d y' + (d+4)\,(s^{d-1}(y^{3/2})')' = 0 \tag{25}$$

We have been unable to find an analytic solution to (25) for any *d;* numerical solutions for the one- and two-dimensional cases are shown in figures 3a) and 4a). The latter figure, derived from

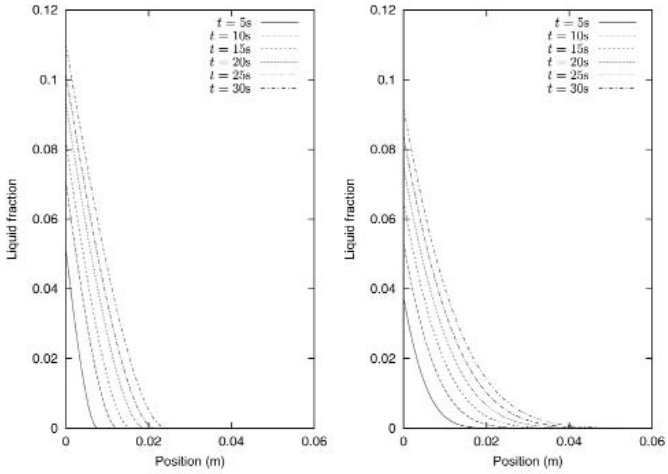

Figure 3: The zero-gravity spreading of a fixed input of liquid introduced into a dry foam in a long, thin, circular tube. Profiles of liquid fraction are shown at various times with input flow-rate q = 30 mm³/s. a) For rigid interfaces, numerically obtained profiles are shown. b) In the case of mobile interfaces the profiles are taken from (29). Notice how they spread more quickly, so that the liquid fraction at the point of input increases less rapidly.

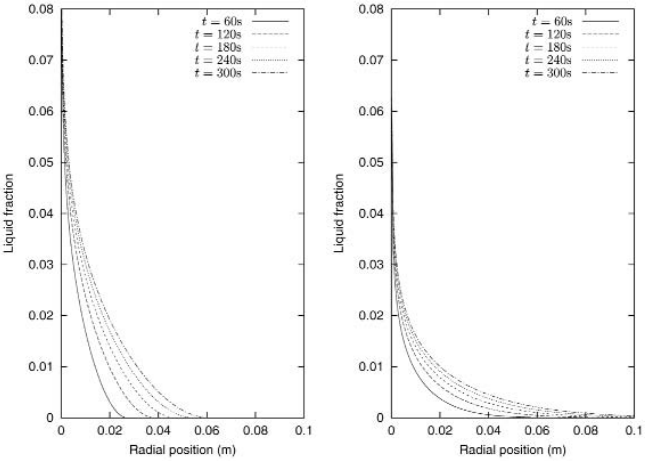

Figure 4: The zero-gravity spreading of a fixed input of liquid introduced into a dry foam between parallel plates. Profiles of liquid fraction in the radial direction are shown at various times with input flow-rate q = 30 mm³/s. a) For rigid interfaces, numerically obtained profiles are shown. b) In the case of mobile interfaces the profiles are taken from (30). Notice how they spread more quickly, so that the liquid fraction at the point of input increases less rapidly.

a numerical simulation, suggests that in 2D (and also in 3D) the solution is singular at the origin. In practice the singularity is eliminated by the introduced liquid being spread over a small region. The numerical solutions allow us to ascertain the dependence of liquid fraction and spreading rate on the input flow-rate Q_0. In 1D we find that the radial position scales with $Q_0^{1/5}$ and that the liquid fraction scales with $Q_0^{4/5}$. Similarly, in 2D we find that position scales as $Q_0^{1/3}$ and liquid fraction scales as $Q_0^{4/5}$ and in 3D position scales as $Q_0^{2/7}$ and liquid fraction scales as $Q_0^{8/7}$.

4.2 Case of mobile interfaces

The flow-rate in this case is taken from (4)

$$Q = -\frac{1}{2}\nabla\alpha = -\frac{1}{2}\frac{\partial\alpha}{\partial\rho} \tag{26}$$

The invariance of Q_0 , as defined above, with time gives $n = 2-d$. Therefore the liquid fraction α scales as

$$\alpha(\rho,\tau) = \tau^{(2-d)/2}(y/s), \quad s = \frac{\rho}{\tau^{1/2}} \tag{27}$$

and we have the same behaviour at the point of input as before - two is the critical dimension in which the liquid fraction remains constant here. The equation for the similarity function (12) becomes

$$(d-s)s^{d-1}y + s^d y' + (s^{d-1}(y))' = 0 \tag{28}$$

Most straightforward is the solution when $d = 1$, for which

$$\alpha(\rho,\tau) = Q_0\left[\sqrt{\frac{2\tau}{\pi}}\,exp\left(-\frac{\rho^2}{2\tau}\right) - \rho\,erfc\left(\frac{\rho}{\sqrt{2\tau}}\right)\right] \tag{29}$$

where erfc is the complementary error function. In 2D, the solution to (28) takes the form of an exponential integral [31]:

$$\alpha(\rho,\tau) = \frac{Q_0}{2\pi}Ei\left(\frac{\rho^2}{2\tau}\right) \tag{30}$$

while in 3D it is a complementary error function [31]:

$$\alpha(\rho,\tau) = \frac{Q_0}{2\pi\rho}erfc\left(\frac{\rho}{\sqrt{2\tau}}\right). \tag{31}$$

Note the singularity at the origin $\rho = 0$ in both 2D and 3D, as for the rigid interface case.

4.3 Dimensional comparison of fixed-input profiles

To illustrate the movement of liquid away from the point of input, we consider a long, thin, circular tube of radius R = 10 mm, as in figure 1a). We introduce liquid uniformly across the plane at position $x = 0$ with dimensional flow-rate q = 30 mm³/s = $Q_0\pi x_0 R^2/t_0$. In dimensional variables the position is $x = x_0 Q_0^{1/5}\rho$ and time is $t = t_0\tau$. The profiles of liquid fraction along the centre-line of the tube are shown in figure 3. Note how, in 1D, the foam gets progressively wetter at the origin - in 2D and 3D experiments this is not the case. For example, in 2D we consider two plates a distance H = 2 mm apart, shown in figure 1b). Liquid is introduced at the origin with dimensional flow-rate q = $Q_0 x_0^2 H/t_0$ = 30 mm³/s. The dimensional position is now $x = x_0 Q_0^{1/3}\rho$. Profiles of liquid fraction are shown in figure 4. Close to the origin the liquid fraction doesn't vary, as predicted, although mathematically there is a singularity at $x = 0$.

5. A step in liquid fraction

We consider next the evolution of an abrupt change in liquid fraction. For instance, what happens when a dry 3D foam is brought into contact with a wet foam? Under the influence of capillary forces the liquid fraction changes so as to wet the dry part of the foam. We analyze this problem in only 1D with position ξ: a higher-dimensional analysis is very similar, but in 1D we obtain the critical information pertaining to the rate at which liquid spreads into the dry foam. The initial condition is

$$\alpha(\xi,\tau=0) = \begin{cases}\alpha_0^l & \xi < 0\\ \alpha_0^r & \xi \geq 0\end{cases} \tag{32}$$

for some fixed liquid fractions $\alpha_0^r < \alpha_0^l$. An initially dry foam for $\xi \geq 0$ corresponds to α_0^r=0

5.1 Case of rigid interfaces

In 1D the diffusion equation (6) is

$$\frac{\partial\alpha}{\partial\tau} = \frac{\partial}{\partial\xi}\left(\frac{\sqrt{\alpha}}{2}\frac{\partial\alpha}{\partial\xi}\right). \tag{33}$$

The liquid fraction is fixed as $\xi \to \pm\infty$ so the scaling parameter is $m = 2$. Thus α scales according to

$$\alpha(\xi,\tau) = y(s), \quad s = \frac{\xi}{\tau^{1/2}} \tag{34}$$

showing that the wetting front moves in the positive ξ-direction with a rate proportional to the square root of time. The solution for the liquid fraction is to be found from (8) with $m = 2$ so that y satisfies

$$sy' + \frac{2}{3}(y^{3/2})^n = 0 \tag{35}$$

Profiles of liquid fraction calculated numerically from (35) are shown in figure 5a), in dimensional variables. Note the fixed

point at $\xi = 0$. We can express this spreading using a diffusion coefficient, which scales as

$$D = \frac{x_0^2}{t_0} = 2.85 \text{x} 10^{-5}\, m^2\, s^{-1}$$

As α_0^r increases from zero, the speed at which the wetting front moves increases; this is analogous to the way a solitary wave moves more rapidly through a wet foam under terrestrial conditions.

5.2 Case of mobile interfaces

For an initial step function in liquid fraction in this case, we have a well-known problem whose solution is an error function:

$$\alpha(\xi,\tau) = \alpha_0^r + \frac{1}{2}(\alpha_0^l - \alpha_0^r) erfc\left(\frac{\xi}{\sqrt{2\tau}}\right) \qquad (36)$$

This solution is shown in figure 5b) to allow comparison with the case of rigid interfaces. Unlike the sharp front (which shows a discontinuity in the second derivative of liquid fraction with respect to position) in the previous case, the dry foam is rapidly wetted everywhere, although in both cases the volume of liquid in moving into the dry region increases in proportion to the square root of time. In this case the diffusion coefficient is

$$D = \frac{x_0^2}{t_0} = 9.94 \text{x} 10^{-6}\, m^2\, s^{-1}$$

which is slightly lower than the value for rigid interfaces.

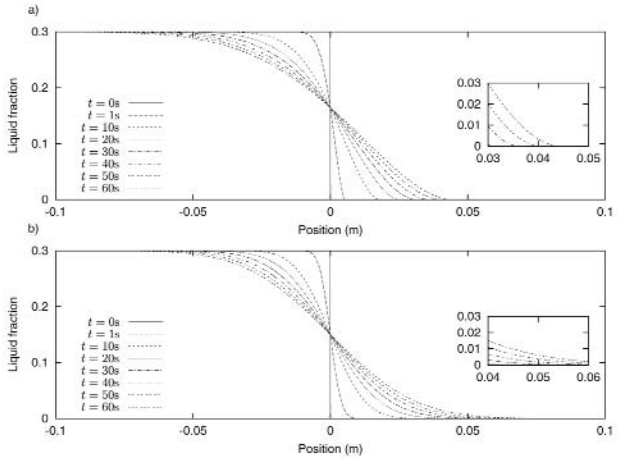

Figure 5: The 1D zero-gravity spreading of a step in liquid fraction into a dry foam. The right-hand side is initially dry (Φ_t=0) and the left-hand side has initial liquid fraction Φ_t=30%. a) In the case of rigid interfaces, numerically obtained profiles are shown for various times. b) Equation (36) gives the profiles for mobile interfaces, which wets the dry foam more rapidly. The insets show the detailed structure of the wetting fronts. Notice the asymmetry of both plots, the fixed point at the origin and the wetting front moving to the right. The volume of liquid in the dry region of time in both cases.

6. A dry foam in contact with a liquid reservoir

Consider now a dry foam which is wetted at one end, for example a dry foam placed in contact with a pool of liquid. The capillary forces will cause liquid to move into the foam, as shown by Caps et al. [12] in parabolic flight experiments. So we put $\alpha(\xi = 0, \tau) = \alpha_0$ and again consider only 1D analysis, although other cases are similar. The parameter $\alpha_0 \approx 35\%$ represents the critical liquid fraction at which the foam becomes a bubbly liquid.

6.1 Case of rigid interfaces

Since α_0 is fixed, we have the same scaling as for the step function initial condition (34), so the wetting front moves away from the pool with the square root of time. The similarity function again satisfies (35), but note that there are slightly different boundary conditions. The amount of liquid in the foam also increases with $\sqrt{\tau}$, with a similar diffusion coefficient to the step-function problem. A numerical solution for the liquid fraction is shown in figure 6.

6.2 Case of mobile interfaces

For the case of liquid moving into a dry foam, the solution is almost identical to the step function problem

$$\alpha(\xi,\tau) = \alpha_0 erfc\left(\frac{\xi}{\sqrt{2\tau}}\right) \qquad (37)$$

where the base of the foam is at $\xi = 0$. This is shown in figure 6; comparison with the case of rigid interfaces suggests that the bulk of the liquid moves more slowly into the dry foam. However, the volume of liquid in the foam also increases in proportion to the square root of time.

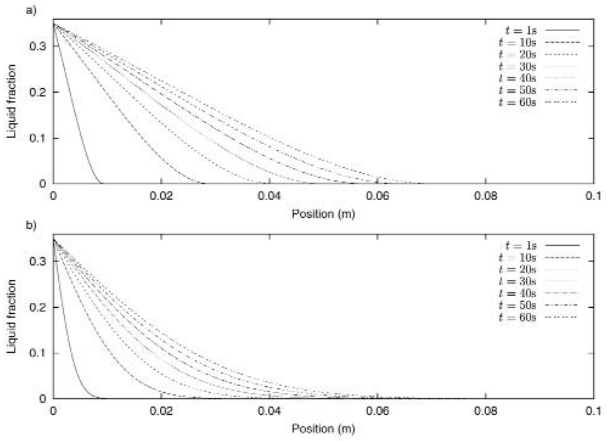

Figure 6: The zero-gravity wetting, with Φ_t= 35% of a 1D dry foam. a) Numerically obtained profiles in the case of rigid interfaces are shown at various times t . b) For the case of mobile interfaces, profiles are obtained from (37). The volume of liquid in the foam increases with the square root of time in both cases, but the constant of proportionality (i.e. the diffusion coefficient) is slightly lower for mobile interfaces.

7. Conclusions

We have solved, using a combination of analysis and numerics, the *d*-dimensional diffusion equation describing the motion of liquid in an aqueous foam under zero-gravity conditions:

$$\frac{\partial \alpha}{\partial \tau} = \frac{1}{2\chi + 1} \nabla^2 \alpha^{\chi + 1/2} \tag{38}$$

in the two limiting cases of $\chi = 1$ (rigid interfaces) and $\chi = 1/2$ (mobile interfaces) [13]. The solutions pertain to four experiments of interest, allowing the rate of spread of the wet regions of the foam to be found in each case. In the case of rigid interfaces these are

- A spreading pulse: the front spreads with $r_o \sim t^{2/(d+4)}$;
- Constant input: the front moves with $r_o \sim t^{3/(d+4)}$;
- A step in liquid fraction / capillary wetting: in both experi ments the front moves into the dry foam with $r_o \sim t^{1/2}$.

The latter solutions show the same behaviour as for mobile interfaces, which always show spreading with the square-root of time. However the fronts are sharper in the case of rigid interfaces and may be easier to measure in practice. This theory now requires comparison with actual experiments. We have described only the limiting cases of high and low interfacial mobility, so are entitled to expect behaviour intermediate between these two extremes. Therefore a careful choice of surfactant may help in performing a meaningful comparison, for example by using a detergent that gives rigid interfaces. Such a programme of experimental work is currently being undertaken under the auspices of the European Space Agency [32]. While intended to use the facilities aboard the International Space Station, the work first aims to pin-point effective foaming devices and suitable test geometries through extensive testing in parabolic flights. The final choice of foam cell is expected to be almost two-dimensional, not least because of ease of visualization and comparison with theory.

Acknowledgements

The authors wish to thank D. Weaire for useful suggestions and discussion. This research was supported by the Prodex and ELIPS programmes of ESA, and is a contribution to ESA contract C14308 / AO-075-99. SJC was partially supported by a Marie Curie fellowship.

References

[1] *D. Weaire and S. Hutzler*. 1999. The Physics of Foams. Clarendon Press, Oxford.
[2] *D. Weaire, S. Hutzler, G. Verbist and E. Peters.* 1997. A review of foam drainage. Advances in Chemical Physics 102:315–374.
[3] *S.A. Koehler, S. Hilgenfeldt and H.A. Stone*. 2000. A generalized view of foam drainage: Experiment and theory. Langmuir 16:6327–6341.
[4] *J.Banhart.* 1999. Foam metal: The recipe. Europhys. News January/February:17–20.
[5] *J. Banhart and D. Weaire.* 2002. On the road again: metal foams find favor. Physics Today July: 37–42.
[6] *S.J. Cox, G. Bradley and D. Weaire.* 2001. Metallic foam processing from the liquid state: the competition between solidification and drainage. Euro. J. Phys: Appl. Physics 14: 87–97.
[7] *D.A. Noever.* 1994. Foam Fractionation of Particles in Low Gravity. J. Spacecraft Rockets 31: 319–322.
[8] *D.A. Noever and R.J. Cronise.* 1994. Weightless bubble lattices: A case of froth wicking. Phys. Fluids 6:2493–2500.
[9] *C. Monnereau and M. Vignes-Adler.* 1998. Dynamics of real three dimensional foams. Phys. Rev. Lett. 80:5228–5231.
[10] *C. Monnereau, M. Vignes-Adler and B. Kronberg.* 1999. Influence of gravity on foams. J. Chim. Phys. 96:958–967.
[11] *T. Wübben, J. Banhart and S. Odenbach.* 2002. Production of metallic foam under low gravity conditions during parabolic flights. Microgravity Sci.Tech. 13:36–42.
[12] *H. Caps, H. Decauwer, M.-L. Chevalier, G. Soyez, M. Ausloos, and N. Vandewalle.* 2003. Foam imbibition in microgravity. Euro. Phys. J. B, 33:115–119.
[13] *S.A. Koehler, S. Hilgenfeldt and H.A. Stone.* 2001. Flow along two-dimensions of liquid pulses in foams: Experiment and theory. Europhys. Lett. 54:335–341.
[14] *S.J. Cox, D.Weaire, S. Hutzler, J. Murphy, R. Phelan and G. Verbist.* 2000. Applications and Generalizations of the Foam Drainage Equation. Proc. R. Soc. Lond. A 456:2441–2464.
[15] *R.A. Leonard and R. Lemlich*. 1965. A Study of Interstitial Liquid Flow in Foam. A.I.Ch.E. J. 11:18–29
[16] *I.I. Goldfarb, K.B. Kann and I.R. Schreiber.* 1988. Liquid flow in foams. Fluid Dynamics 23: 244–249.
[17] *G. Verbist, D. Weaire and A.M. Kraynik*. 1996. The foam drainage equation. J. Phys.:Condensed Matter 8:3715–3731.
[18] *S.J. Cox, G. Bradley, S. Hutzler and D. Weaire.* 2001. Vertex corrections in the theory of foam drainage. J. Phys: Condens. Matter 13:4863–4869.
[19] *S.A. Koehler, S. Hilgenfeldt and H.A. Stone.* 1999. Liquid flow through aqueous foams: The node-dominated foam drainage equation. Phys. Rev. Lett. 82:4232–4235.
[20] *M. Durand, G. Martinoty and D. Langevin.* 1999. Liquid flow through aqueous foams: From the Plateau border-dominated regime to the node-dominated regime. Phys. Rev. E 60:R6307 – R6308.
[21] *A. Saint-Jalmes, and D. Langevin*, 2002. Time evolution of aqueous foams: drainage and coarsening. J. Phys.: Condens. Matter 14: 9397–9412.
[22] *S. A. Koehler, S. Hilgenfeldt, E. R. Weeks, and H. A. Stone,* 2002. Drainage of single plateau borders: direct observation of rigid and mobile interfaces. Phys. Rev. E 66:040601.
[23] *A.M. Kraynik.* 1983. Foam Drainage. Sandia Report (SAND83-0844).
[24] *M. Durand and D. Langevin.* 2002. Physicochemical approach to the theory of foam drainage. Eur. Phys. J. E 7:35–44.
[25] *S.A. Koehler, H.A. Stone, M.P. Brenner and J. Eggers.* 1998. Dynamics of foam drainage. Phys. Rev. E 58:2097–2106.
[26] *G.I. Barenblatt.* 1996. Scaling, self-similarity, and intermediate asymptotics. Cambridge University Press.
[27] *L. Dresner.* 1983. Similarity solutions of nonlinear partial differential equations. Pitman, Boston.
[28] *D. Weaire, N. Pittet, S. Hutzler and D. Pardal.* 1993. Steady-state draina ge of an aqueous foam. Phys. Rev. Lett. 71:2670–2674.
[29] *Vera, M.U. and Durian, D.J.* 2002. Enhanced drainage and coarsening in aqueous foams. Phys. Rev. Lett. 88:088304.
[30] *C.J. Budd and G.J. Collins.* 1998. An invariant moving mesh scheme for the nonlinear diffusion equation. Appl. Num. Math. 26:23–29.
[31] *H.S. Carslaw and J.C. Jaeger.* 1959. Conduction of Heat in Solids. Clarendon, Oxford.
[32] *D. Langevin.* 2002. Hydrodynamics of Wet Foams. ESA contract AO-99-108.